HHS Public Access

Author manuscript

FASEB J. Author manuscript; available in PMC 2022 February 01.

Published in final edited form as:

FASEB J. 2021 February ; 35(2): e21272. doi:10.1096/fj.202001782RR.

Protective role of IL33 signaling in negative pregnancy outcomes associated with lipopolysaccharide exposure

Keisuke Kozai[1], **Khursheed Iqbal**[1], **Ayelen Moreno-Irusta**[1], **Regan L. Scott**[1], **Mikaela E. Simon**[1], **Pramod Dhakal**[1], **Patrick E. Fields**[1], **Michael J. Soares**[1,2,3,4]

[1]Institute for Reproduction and Perinatal Research, Department of Pathology & Laboratory Medicine, University of Kansas Medical Center, Kansas, KS, USA

[2]Department of Pediatrics, University of Kansas Medical Center, Kansas, KS, USA

[3]Department of Obstetrics and Gynecology, University of Kansas Medical Center, Kansas, KS, USA

[4]Center for Perinatal Research, Children's Mercy Research Institute, Children's Mercy, Kansas, MO, USA

Abstract

Interleukin 33 (IL33) signaling has been implicated in the establishment and maintenance of pregnancy and in pregnancy disorders. The goal of this project was to evaluate the role of IL33 signaling in rat pregnancy. The rat possesses hemochorial placentation with deep intrauterine trophoblast invasion; features also characteristic of human placentation. We generated and characterized a germline mutant rat model for IL33 using CRISPR/Cas9 genome editing. IL33 deficient rats exhibited deficits in lung responses to an inflammatory stimulus (Sephadex G-200) and to estrogen-induced uterine eosinophilia. Female rats deficient in IL33 were fertile and exhibited pregnancy outcomes (gestation length and litter size) similar to wild-type rats. Placental weight was adversely affected by the disruption of IL33 signaling. A difference in pregnancy-dependent adaptations to lipopolysaccharide (LPS) exposure was observed between wild-type and IL33 deficient pregnancies. Pregnancy in wildtype rats treated with LPS did not differ significantly from pregnancy in vehicle-treated wild-type rats. In contrast, LPS treatment decreased fetal survival rate, fetal and placental weights, and increased fetal growth restriction in IL33 deficient rats. In summary, a new rat model for investigating IL33 signaling has been established. IL33 signaling participates in the regulation of placental development and protection against LPS-induced fetal and placental growth restriction.

Correspondence Keisuke Kozai and Michael J. Soares, Department of Pathology and Laboratory, Medicine, University of Kansas Medical Center, 3901 Rainbow Boulevard, Kansas, KS 66160, USA., kkozai@kumc.edu, msoares@kumc.edu.
Present address Pramod Dhakal, Animal Science Research, Center, Division of Animal Sciences, University of Missouri, Columbia, MO, USA

AUTHOR CONTRIBUTIONS

K. Kozai, K. Iqbal, P.E Fields, and M.J. Soares designed the research; K. Kozai, K. Iqbal, and M.J. Soares analyzed the data; K. Kozai, K. Iqbal, A. Moreno-Irusta, R.L. Scott, M.E. Simon, and P. Dhakal performed the research; K. Kozai and M.J. Soares wrote the paper. All authors participated in editing the manuscript.

SUPPORTING INFORMATION

Additional Supporting Information may be found online in the Supporting Information section.

Keywords

fetal growth restriction; IL33; lipopolysaccharide; pregnancy outcome; placental development

1 | INTRODUCTION

During the establishment of pregnancy, the uterus undergoes a profound transformation. Uterine stromal cells differentiate into decidual cells, while uterine glands and blood vessels exhibit structural and functional modifications, and immune cells are systematically recruited, redistributed, or excluded from the endometrium.[1–3] The biology of immune cells within the uterus has been the focus of a significant body of research.[2,3] Natural killer cells, macrophages, dendritic cells, and T-regulatory cells each possess pivotal regulatory roles in the establishment of pregnancy and hemochorial placentation.[4–13] Immune cells also contribute to uterine inflammatory responses during embryo implantation.[14–16] As pregnancy progresses, the uterine T helper 1 (Th1) cell and T helper 2 (Th2) cell cytokine milieu undergoes changes essential for embryo implantation, maintenance of pregnancy, and parturition.[17–19] Excessive inflammation during pregnancy has been implicated in negative pregnancy outcomes.[16,18] Lipopolysaccharide (LPS) is an effective trigger of inflammatory states in animal models.[20–24] LPS exposure during pregnancy can yield negative pregnancy outcomes, including fetal growth restriction,[20] preterm labor,[21,22] and pregnancy loss.[23,24] Modulation of uterine immune and inflammatory cell populations during the course of gestation is poorly understood.

Interleukin 33 (IL33) is a member of the interleukin 1 (IL1) family of cytokines and a key modulator of innate immunity.[25–29] IL33 resides in the nucleus of its cellular source (eg, endothelial and epithelial cells) and is liberated to the extracellular milieu upon specific changes in the cellular environment.[26,27,29] Suppressor of tumorigenicity 2 (ST2) is the common name for the IL33 receptor, which is officially termed IL1 receptor-like 1 (IL1RL1). ST2 is abundantly expressed on innate lymphoid cells, Th2 cells, subsets of regulatory T cells, and an assortment of other immune cells.[26,29] IL33 possesses important immune cell modulatory roles in tissue homeostasis following infection, allergy, and inflammatory disease[26,29] and contributes to the regulation of thermogenesis.[30] Interestingly, the known involvement of IL33 in tissue homeostasis associated with inflammation and its modulatory role in Th2 cell cytokine biology places it in a potentially intriguing position for modulating immune cell events within the uterus during pregnancy.

IL33 and ST2 are expressed at the maternal-fetal interface.[31–38] Disruptions of IL33 signaling have been connected to diseases of pregnancy and placentation. Both recurrent pregnancy loss and preeclampsia are associated with aberrations in IL33 and/or ST2 function.[31–43] Furthermore, IL33 signaling has been implicated as a regulator of intrauterine immune cell events at the end of gestation preceding parturition.[43] The majority of these observations are correlative and place IL33 and ST2 in a provocative position as a potential regulator of pivotal gestational events.

In this report, we examine a role for IL33 signaling in pregnancy outcomes using a genome edited *loss-of-function* rat model. The rat is a useful model for investigating pregnancy and

deep placentation, as these events show many similarities to those observed in the human.[44–46] We show that IL33 signaling impacts pregnancy outcomes and serves a protective role in LPS exposed pregnancies.

2 | MATERIALS AND METHODS

2.1 | Animals

The Holtzman Sprague Dawley rat was used in the experimentation described in this report. Holtzman Sprague Dawley rats possess robust fertility (litter sizes ranging from 12–15 pups), are easy to handle, and have been used extensively in pregnancy-related research.[46,47] Rats were maintained in an environmentally controlled facility with lights on from 0600 to 2000 hours with food and water available ad libitum. Time-mated pregnancies were established by co-housing adult female rats (8–10 weeks of age) with adult male rats (>10 weeks of age). Detection of sperm or a seminal plug in the vagina was designated gestation day (gd) 0.5. Pseudopregnancies were generated by co-housing adult female rats (8–10 weeks of age) with adult male vasectomized males (>10 weeks of age). Detection of seminal plugs were designated pseudopregnancy day 0.5. Four- to five-week-old donor rats were intraperitoneally injected with 30 units of pregnant mare serum gonadotropin (cat. no. G4877, Sigma-Aldrich, St. Louis, MO), followed by an intraperitoneal injection of 30 units of human chorionic gonadotropin (cat. no. C1063, Sigma-Aldrich) ~46 hours later, and then, immediately mated. Zygotes were flushed from oviducts the next morning (gd 0.5). The University of Kansas Medical Center Animal Care and Use Committee approved all protocols involving the use of rats.

2.2 | Placentation site dissections and processing

Whole placentation sites were dissected and processed as previously described.[47] Tissues were placed into dry ice-cooled heptane and stored at −80°C until processed for immunohistochemical or in situ hybridization analyses. Alternatively, placentation sites were dissected into components, including the fetus, placenta, and metrial gland. In other instances, the placenta was further dissected into junctional and labyrinth zone compartments. Fetuses and placentas were routinely assessed for viability and weighed. Dissected placentation site components were frozen in liquid nitrogen and stored at −80°C until used for biochemical assessments.

2.3 | Generation of an *Il33* mutant rat model

Mutations of the *Il33* locus were generated using CRISPR/ Cas9 genome editing.[13,32,48,49] Guide RNAs targeting Exon 3 (target sequence: TACTGCATGAGGCTCCGTTC; nucleotides 196–215) and Exon 8 (target sequence: TGATGTCTCTCCGCCAGATC; nucleotides 678–697) of the rat *Il33* gene (NM_001014166.1) were microinjected into single-cell rat embryos. Injected embryos were transferred to oviducts of day 0.5 pseudopregnant rats. Initially, offspring were screened for mutations at specific target sites within the *Il33* gene via isolating genomic DNA from tailtip biopsies using the REDExtract-N-Amp Tissue PCR kit (XNAT, Millipore Sigma, Burlington, MA). Polymerase chain reaction (PCR) was performed on the purified DNA samples using primers flanking the guide RNA sites (Forward primer: CCCTCCATAAAGGACTTGAG, Reverse primer:

GCCTTTCTTCAGTTGGAAG), and products resolved by agarose gel electrophoresis and ethidium bromide staining. Genomic DNA containing potential mutations was amplified by PCR, gel purified, and precise boundaries of deletions determined by DNA sequencing (Genewiz Inc, South Plainfield, NJ). Founders with *Il33* mutations were backcrossed to wildtype rats to demonstrate germ line transmission. Routine genotyping was performed by PCR on genomic DNA with a specific set of primers (Forward: CCCTCCATAAAGGACTTGAG, Reverse-1: CATCATCCCATAGGATTACATG, Reverse-2: GCCTTTCTTCAGTTGGAAG). The *Il33* mutant rat model is available at the Rat Resource & Research Center (RRRC No. 883; University of Missouri, Columbia, MO; www.rrrc.us).

2.4 | Western blot analysis

Tissue lysates were prepared with Radioimmunoprecipitation Assay Lysis Buffer System (cat. no. sc-24948A, Santa Cruz Biotechnology, Santa Cruz, CA). Protein concentrations were determined using the *DC*™ Protein Assay Kit (Cat. No. 5000112, Bio-Rad Laboratories, Hercules, CA). Proteins (20 μg) were separated by SDS-PAGE. Separated proteins were electrophoretically transferred to polyvinylidene difluoride membranes (cat. no. 10600023, GE Healthcare, Milwaukee, WI) for 1 hour at 100 V on ice. Membranes were subsequently blocked with 5% milk for 1 hour at room temperature and probed separately with specific primary antibodies to IL33 (1:1,000 dilution, cat. no. ALX-804–840-C100, Enzo Life Sciences, Inc, Farmingdale, NY), uncoupling protein 1 (UCP1; 1:10,000 dilution, cat. no. ab10983, Abcam, Cambridge, MA), or glyceraldehyde 3-phosphate dehydrogenase (GAPDH, 1:5,000 dilution, cat. no. ab8245, Abcam) in Tris-buffered saline with Tween 20 (TBST) overnight at 4°C. After primary antibody incubation, the membranes were washed in TBST three times for 10 minutes each at room temperature. After washing, the membranes were incubated with anti-mouse immunoglobulin G (IgG) conjugated to horseradish peroxidase (HRP, 1:5,000 dilution, cat. no. 7076S, Cell Signaling Technology, Danvers, MA) in TBST for 1 hour at room temperature, washed in TBST three times for 10 minutes each at room temperature, immersed in Immobilon Crescendo Western HRP Substrate (cat. no. WBLUR0500, Sigma-Aldrich), and luminescence detected using Radiomat LS film (Agfa Healthcare, Mortsel, Belgium).

2.5 | Sephadex-induced rat pulmonary inflammation

Pulmonary inflammation was induced as described previously.[50–52] Briefly, a suspension of Sephadex G-200 (Sephadex; Chemsavers, Bluefield, VA) was prepared in sterile saline at a concentration of 0.5 mg/mL and stored for at least 48 hours at 4°C with gentle stirring and autoclaved before administration. Male rats (6–7 weeks of age) were injected intravenously via the tail vein with sterile saline (1 mL/animal) or Sephadex (0.5 mg/mL/animal) on days 0 and 2 and sacrificed on day 5. Lungs were excised and either placed into dry ice-cooled heptane or frozen in liquid nitrogen and stored at −80°C for subsequent eosinophil peroxidase (EPO) histochemical analysis or assessment of transcript expression (see below), respectively.

2.6 | Estrogen-induced uterine eosinophilia

Treatment of prepubertal female rats with estrogen is a reproducible method for the experimental induction of uterine eosinophilia.[53,54] Prepubertal female rats were subcutaneously injected with sesame oil (100 μL/animal) or estradiol benzoate (10 μg/100 μL sesame oil/animal, cat. no. 10006487, Cayman Chemical, Ann Arbor, MI) daily from postnatal day (PND) 20 through PND 22 and sacrificed on PND 23. Uteri were removed and placed into dry ice-cooled heptane and stored at −80°C until processed for histochemical analysis.

2.7 | EPO histochemical analysis

Cyanide-resistant EPO histochemical analysis was performed as described previously.[55,56] Briefly, frozen sections (10 μm) from lungs, uteri, or placentation sites were stained for 30 minutes at room temperature using 3-amino-9-ethylcarbazole (AEC) peroxidase substrate solution (cat. no. SK-4200, Vector Laboratories, Burlingame, CA) containing 8 mM NaCN (cat. no. 380970, Sigma-Aldrich). Stained sections were washed for 5 minutes with Hank's Balanced Salt Solution, and counterstained with VECTOR Hematoxylin QS (cat. no. H-3404, Vector Laboratories, Burlingame, CA), and examined microscopically.

2.8 | Analysis of brown adipose tissue

At 3 weeks of age brown adipose tissue was dissected from the scapular region of male *Il33*$^{+/+}$ or *Il33*$^{-/-}$ rats, weighed, and UCP1 protein assessed by western blotting.

2.9 | Transcript analysis

2.9.1 | Reverse transcription-quantitative PCR (RT-qPCR)—Total RNA was extracted from tissues using TRI Reagent Solution (cat. no. AM9738, Thermo Fisher, Waltham, MA) according to the manufacturer's instructions. Total RNA (1 μg) was reverse transcribed using High-Capacity cDNA Reverse Transcription Kit (cat. no. 4368813, Thermo Fisher). Complementary DNAs were diluted 1:10 and subjected to RT-qPCR using PowerUp SYBR Green Master Mix (cat. no. A25742, Thermo Fisher) and primers described in Table 1. QuantStudio 7 Flex Real-Time PCR System (Applied Biosystems, Foster City, CA) was used for amplification and fluorescence detection. PCR was performed under the following conditions: 95°C for 10 minutes, followed by 40 cycles of 95°C for 15 s, and 60°C for 1 minute. Relative mRNA expression was calculated using the delta-delta Ct method. *Gapdh* was used as a reference transcript.

2.9.2 | In situ hybridization—Detection of transcripts for *Il33*, *Acta2*, *Adgrl4*, *Prl7b1*, and *Lyz2* was performed on cryosections of rat placentation sites. *Acta2*, *Adgrl*4, *Prl7b1*, and *Lyz2* were used to identify smooth muscle, endothelial, invasive trophoblast cells, and macrophages, respectively. The RNAscope Multiplex Fluorescent Reagent Kit version 2 (Advanced Cell Diagnostics, Newark, CA) was used for the in situ hybridization analysis, according to the manufacturer's instructions. Probes were prepared to detect *Il33* (NM_001014166.1, cat no. 449578, target region: 2–983), *Acta2* (NM_031004.2, cat. no. 421501-C2, target region: 5–1361), *Adgrl4* (NM_022294.1, cat. no. 878411-C2, target region: 886–1871), *Prl7b1* (NM_153738.1, cat no. 860181-C2, target region: 28–900), and

Lyz2 (NM_012771.3, cat. no. 888811-C2, target region: 82–1181). Fluorescence images were captured on a Nikon 80i upright microscope (Nikon, Melville, NY) with a Photometrics CoolSNAP-ES monochrome camera (Roper, Sarasota, FL).

2.10 | LPS treatment of pregnant rats

Pregnant rats were treated with LPS to establish an inflammatory state as previously reported.[20] Rats were injected intraperitoneally with sterile saline (1 mL/kg body weight, daily from gd 13.5 through gd 16.5) or LPS (cat. no. L3129, *Escherichia coli* serotype O127:B8; Sigma-Aldrich: 10 μg/ mL/kg body weight on gd 13.5, followed by 60 μg/mL/kg body weight daily until gd 16.5) and sacrificed on gd 17.5. The LPS solution was prepared in sterile saline. Rats received Ringer's lactate solution (5 mL/kg) subcutaneously with each injection.

2.11 | Immunohistochemistry

Placentation sites were embedded in OCT compound and sectioned at 10 μm thickness. Sections were fixed in 4% paraformaldehyde, washed in phosphate-buffered saline (pH 7.4) three times for 5 minutes each, blocked with 10% Normal Goat Serum (cat. no. 50062Z, Thermo Fisher), and incubated overnight with a mouse monoclonal anti-pan cytokeratin antibody conjugated with fluorescein isothiocyanate (1:300 dilution; cat. no. F3418, Sigma-Aldrich) to identify trophoblast cells, or with a mouse monoclonal anti-vimentin antibody (1:300 dilution; cat. no. sc-6260, Santa Cruz Biotechnology) to distinguish placental compartments followed by incubation with anti-mouse IgG conjugated to HRP (1:500 dilution, cat. no. A9044, Sigma-Aldrich) for 3 hours at room temperature and color development with an AEC substrate kit (cat. no. SK4200, Vector Laboratories). Sections were then mounted with Fluoromount-G mounting media (cat. no. 0100–01, SouthernBiotech, Birmingham, AL) and examined microscopically. Fluorescence images were captured on a Nikon 80i upright microscope (Nikon) with a Photometrics CoolSNAP-ES monochrome camera (Roper). The area occupied by cytokeratin-positive cells (invasive trophoblast cells) within the metrial gland was quantified using ImageJ software, as previously described.[57]

2.12 | Statistical analysis

Student's *t* test, Welch's *t* test, Dunnett's test, or Fisher's Exact test were performed, where appropriate, to evaluate the significance of the experimental manipulations. Results were deemed statistically significant when $P < .05$.

3 | RESULTS

3.1 | Generation of an *Il33* mutant rat model

CRISPR/Cas9 genome editing was used to generate a mutant rat strain possessing a 6,691 base pair deletion within the *Il33* gene, which included part of Exon 3, the entire region spanning Exon 4 through Exon 7, and part of Exon 8 (Figure 1). The deletion led to a frameshift and premature stop codon, resulting in a disruption of the IL33 protein (Figure 1). Sequencing of cDNA from *Il33* homozygous mutant lung RNA verified the integrity of the genomic deletion. The *Il33* mutation was successfully transmitted through the germline and

a mutant *Il33* rat colony established and maintained via heterozygous x heterozygous breeding. Mating of heterozygotes produced the expected Mendelian ratio for the *Il33* mutant model (Table 2).

3.2 | Biological validation of IL33 deficiency

IL33 signaling is involved in tissue eosinophilia and Th2 cell responses to inflammatory stimuli.[58–62] In order to biologically validate our IL33 rat model, we used two models for inducing eosinophilia: Sephadex-induced lung eosinophilia and estrogen-induced uterine eosinophilia.

We treated *Il33* mutant rats and wild-type control rats (littermates) with Sephadex, which has been shown to induce pulmonary inflammation characterized by profound eosinophilia and Th2 cytokine upregulation in rats.[50–52,63] Sephadex-induced lung eosinophilia was attenuated in IL33 deficient rats, as was lung expression of transcripts for Th2 cytokines, interleukin 5 (*Il5*) and interleukin 13 (*Il13*, Figure 2). Eosinophil distributions within the uteri of estrogen-treated wild-type and IL33 deficient rats were also evaluated. Estrogen treatment elicited a dramatic accumulation of eosinophils in the uteri of wild-type rats, but not in IL33 deficient rats (Figure 3). The absence of these inflammatory responses in IL33 deficient rats provides strong biological evidence supporting the efficacy of our disruption of the *Il33* locus.

3.3 | Brown adipose tissue development

An earlier report in mice possessing disruptions at *Il33* and *Il1rl1* loci indicated that brown adipose tissue development was dependent on intact IL33 signaling.[30] In contrast, brown adipose tissue development in the rat was similar with or without an intact IL33 signaling pathway (Figure 4). Brown adipose tissue appearance, weight, and expression of UCP1 protein were similar in $Il33^{+/+}$ and $Il33^{-/-}$ rats.

3.4 | Effects of IL33 deficiency on pregnancy outcome

We next assessed fertility and pregnancy outcomes from rats with deficits in IL33. Homozygous mutant offspring generated from *Il33* heterozygote intercrosses were viable and fertile. Placentas and fetuses generated from heterozygote intercrosses did not exhibit significant gravimetric differences based on genotype. These results prompted an examination of the distribution of *Il33* within the placentation site (Figure 5, Table S1). *Il33* transcripts were prominently expressed in the uterus proximal to the placenta (also referred to as the metrial gland) but not within the placenta. We used in situ hybridization to identify the cellular source of *Il33* transcripts within the metrial gland at gd 17.5. In situ hybridization revealed that *Il33* transcripts were colocalized with *Adgrl1* transcripts (endothelial cells) but not with *Acta2* (smooth muscle cells), *Prl7b1* (invasive trophoblast cells), or *Lyz2* (macrophages) transcripts (Figure 5C, Supporting Figure S1).

Wild type x wild type and $Il33^{-/-}$ x $Il33^{-/-}$ pregnancies were also established. There were no significant effects of the *Il33* null mutation on gestation length, litter size, or fetal weights. However, placental weights were significantly smaller for *Il33* null pregnancies (Figure 6).

The implication from these results is that maternal IL33 signaling contributes to placental development.

3.5 | Role of IL33 signaling in pregnancy adaptations to LPS

IL33 signaling possesses a prominent role in modulating responses to inflammation.[58–62] LPS is routinely used to induce inflammatory states in rats.[20,23,64–67] Consequently, we examined the outcomes for *Il33*$^{-/-}$ or wild-type littermate control pregnancies following exposure to saline or LPS.

There were no differences in placental weights in saline-treated wild-type vs IL33 deficient rats. Additionally, the LPS effects on pregnancy observed in our study with wildtype rats were modest/subthreshold in comparison to previous reports.[20,23,64–67] These differences may be attributed to the LPS treatment protocol, parameters measured, rat strain selection, or environmental influences unique to each investigation. Nevertheless, our results are consistent with IL33 providing protection against the negative effects of LPS exposure. LPS exposure had the most severe adverse effects on placental and fetal weights in pregnancies with impaired IL33 signaling (Figure 7A and B). In the present study, fetuses with fetal growth restriction were defined as fetuses which have a weight below the 10th percentile for gestation age. Consistent with these results, the percentage of fetuses with fetal growth restriction was significantly higher in LPS-treated *Il33*$^{-/-}$ rats than that of any other group (Figure 7C). Fetal survival rate was significantly decreased when *Il33*$^{-/-}$ rats were exposed to LPS (Figure 7D).

The organization of placental compartments was not affected by genotype or LPS treatment (Figure 8A). Impairments were observed in the uterine-placental interface of LPS-treated *Il33*$^{-/-}$ rats. Indices of trophoblast invasion, including cytokeratin staining and expression of *Prl5a1* and *Prl7b1* (invasive trophoblast-specific markers[44,68]) were significantly disrupted in LPS-treated *Il33*$^{-/-}$ rats (Figure 8B, C, D, and E). Expression of Th2 cytokine transcripts (*Il5* and *Il13*) in the uterine-placental interface was low and did not differ between wild-type and IL33 deficient pregnancies. Eosinophils were not detected at the uterine-placental interface.

Collectively, the data indicate that deficits in IL33 signaling adversely affect placental development and pregnancy-dependent adaptations to LPS exposure.

4 | DISCUSSION

It is apparent from a vast and growing literature that IL33 possesses critical actions coordinating immune cell function in a broad range of physiological and pathological processes.[26–28] In this report, we sought to elucidate the involvement of IL33 signaling in the regulation of pregnancy outcomes. We selected the rat as an animal model for evaluating pregnancy outcomes because of parallels in deep hemochorial placentation observed in both the rat and human.[45,46,69] To proceed, we first generated and validated a *loss-of-function* rat model for IL33 using CRISPR/Cas9 genome editing. Disruption of IL33 interfered with lung eosinophilia and Th2 cell responses evoked by a potent inflammatory stimulus and uterine eosinophilia induced by estrogen. Pregnancy outcomes, as measured by viability, litter size,

and duration of pregnancy were not significantly impacted by a deficiency in IL33. Placental weights were adversely affected by disruption of IL33 signaling but other aspects of placentation, including junctional and labyrinth zone development and intrauterine trophoblast invasion, were not affected. Challenging female rats possessing a deficiency in IL33 with LPS led to pregnancy complications characterized by placental and fetal growth restriction, fetal loss, and placental dysplasia. The results implicate IL33 in regulating cellular dynamics at the uterine-placental interface during immune activation.

Disruption of IL33 signaling in the mouse has a profound effect on brown adipose tissue development.[30,70] IL33 was proposed to possess a key role in thermogenesis and vulnerability to cold temperatures. In contrast, a similar disruption in the rat did not adversely affect morphogenesis of brown fat (present study). It is not apparent whether this divergence in IL33 actions reflects a species difference, a strain difference, or whether environmental disparities contributed to differences observed in the mouse and rat.

Some pregnancy outcomes were not affected by IL33 signaling, while other parameters were affected. Viability and litter size did not differ between wild-type rats and rats with IL33 signaling deficiencies. IL33 signaling has previously been implicated in inflammatory processes leading to preterm birth[43] but did not significantly affect gestation length in *Il33*$^{-/-}$ rat pregnancies (present study). Placental weight was sensitive to IL33 signaling. However, the placental gravimetric deficit was not associated with impairments in placental morphogenesis or at least one measure of placental function, fetal weight. Compensatory mechanisms may have been sufficient to normalize the function of the smaller *Il33*$^{-/-}$ placentas. Alternatively, the compromised *Il33*$^{-/-}$ placentas may have impacted parameters of fetal development not examined. *Il33*$^{-/-}$ rat pregnancies possessed global deficiencies in IL33 signaling, including maternal, placental, and fetal compartments. IL33 can be expressed in a number of cell types and tissues. We found the uterine interface proximal to the placenta to be the most abundant source of IL33 within the placentation site. This uterine structure possesses stromal cells, smooth muscle cells, endothelial cells, a wide range of immune cells, including macrophages and natural killer cells, and during the latter stages of gestation, invasive trophoblast cells.[71] A major cellular source of *Il33* within the uterine-placental interface (metrial gland) was cells lining blood vessels. Vasculature-associated *Il33* was co-localized with *Adgrl4*, an endothelial cell-specific transcript,[72,73] but not *Acta2*, *Prl7b*, or *Lyz2* transcripts, which are expressed in smooth muscle,[74,75] invasive trophoblast cells,[44,68] and macrophages,[76] respectively. Thus, a major source of IL33 at the uterine-placental interface appears to be endothelial cells of uterine blood vessels that have not been remodeled by invasive endovascular trophoblast cells. Endothelial cells have been previously shown to be a source of IL33.[25–28] Endothelial cell-derived IL33 has been implicated in responses to vascular remodeling, injury, and inflammation leading to the modulation of endothelial cell permeability, coagulation, cytokine production, and metabolism,[77–80] processes potentially relevant in the establishment of the uterine-placental interface. There is some suggestion that macrophage-derived IL33 may facilitate trophoblast cell proliferation and drive placental growth.[34] Macrophages did not represent a major source of IL33 at gd 17.5 but may be a more prominent contributor to IL33 production at earlier or later stages of pregnancy. Elucidation of any potential involvement of IL33 signaling in placental and fetal

development will require an enhanced cellular and molecular dissection of events associated with the progression of pregnancy.

Interestingly, the importance of IL33 signaling in placental development was obscured by maternal stress. Wild-type vs IL33 mutant differences in placental weights disappeared in pregnant rats receiving daily intraperitoneal injections of saline and Ringer's lactate solution from gd 13.5 to 16.5. During this gestational interval the placenta exhibits approximately a 10-fold increase in growth.[81] Although, not directly tested, it appears that maternal stress may have negatively affected placental growth, which is consistent with earlier observations on the effects of maternal stress on placental growth and function.[82–85] There is abundant evidence that maternal stress affects immune, inflammatory, and developmental processes, including placental morphogenesis.[86–88]

The absence of IL33 signaling adversely affected pregnancy-d ependent adaptations to maternal immune activation. Fetal growth restriction and death were more prevalent in *Il33*$^{-/-}$ pregnancies exposed to LPS. These observations implicate maternal IL33 signaling in fetal responses to maternal infection. A mechanism for IL33 signaling acting in a protective role preventing fetal growth restriction and death induced by LPS exposure is unknown. The negative fetal responses correlated with abnormal placentation, including impairments in intrauterine invasive trophoblast cells. Excessive inflammation has previously been shown to disrupt intrauterine trophoblast invasion, resulting in fetal growth restriction.[44] The experimental platform we have established for investigating the biology of IL33 signaling will provide a new tool for understanding immune cell and inflammatory mechanisms at the uterine-placental interface, including their dysregulation in pregnancy-related diseases.

Supplementary Material

Refer to Web version on PubMed Central for supplementary material.

ACKNOWLEDGMENTS

This work was supported by the Lalor Foundation (KK, AM-I), American Heart Association (KK), NIH grants (HD020676, HD079363, and HD099638), and the Sosland Foundation. The authors also thank Stacy Oxley and Brandi Miller for administrative assistance.

Funding information

Lalor Foundation; American Heart Association; NIH, Grant/Award Number: HD020676, HD079363 and HD099638; Sosland Foundation

Abbreviations:

AEC	3-amino-9-ethylcarbazole
EPO	eosinophil peroxidase
GAPDH	glyceraldehyde 3-phosphate dehydrogenase
gd	gestation day

HRP	horseradish peroxidase
IgG	immunoglobulin G
IL1	interleukin 1
IL33	interleukin 33
IL5	interleukin 5
IL13	interleukin 13
IL1RL1	interleukin 1 receptor-like 1
LPS	lipopolysaccharide
PCR	polymerase chain reaction
PND	postnatal day
ST2	suppressor of tumorigenicity 2
Th1	T helper 1
Th2	T helper 2
TBST	tris-buffered saline with Tween 20
UCP1	uncoupling protein 1

REFERENCES

1. Cha J, Sun X, Dey SK. Mechanisms of implantation: strategies for successful pregnancy. Nat Med. 2012;18:1754–1767. [PubMed: 23223073]
2. Erlebacher A. Immunology of the maternal-fetal interface. Annu Rev Immunol. 2013;31:387–411. [PubMed: 23298207]
3. Zhang J, Dunk C, Croy AB, Lye SJ. To serve and to protect: the role of decidual innate immune cells on human pregnancy. Cell Tissue Res. 2016;363:249–265. [PubMed: 26572540]
4. Pollard JW, Hunt JS, Wiktor-Jedrzejczak W, Stanley ER. A pregnancy defect in the osteopetrotic (op/op) mouse demonstrates the requirement for CSF-1 in female fertility. Dev Biol. 1991;148:273–283. [PubMed: 1834496]
5. Guimond MJ, Luross JA, Wang B, Terhorst C, Danial S, Croy BA. Absence of natural killer cells during murine pregnancy is associated with reproductive compromise in TgE26 mice. Biol Reprod. 1997;56:169–179. [PubMed: 9002646]
6. Aluvihare VR, Kallikourdis M, Betz AG. Regulatory T cells mediate maternal tolerance to the fetus. Nat Immunol. 2004;5:266–271. [PubMed: 14758358]
7. Krey G, Frank P, Shaikly V et al. In vivo dendritic cell depletion reduces breeding efficiency, affecting implantation and early placental development in mice. J Mol Med (Berl). 2008;86:999–1011. [PubMed: 18575833]
8. Plaks V, Birnberg T, Berkutzki T et al. Uterine DCs are crucial for decidua formation during embryo implantation in mice. J Clin Invest. 2008;118:3954–3965. [PubMed: 19033665]
9. Collins MK, Tay CS, Erlebacher A. Dendritic cell entrapment within the pregnant uterus inhibits immune surveillance of the maternal/fetal interface in mice. J Clin Invest. 2009;119:2062–2207. [PubMed: 19546507]

10. Chakraborty D, Rumi MA, Konno T, Soares MJ. Natural killer cells direct hemochorial placentation by regulating hypoxia-inducible factor dependent trophoblast lineage decisions. Proc Natl Acad Sci USA. 2011;108:16295–16300. [PubMed: 21900602]
11. Rowe JH, Ertelt JM, Aguilera MN, Farrar MA, Way SS. Foxp3(+) regulatory T cell expansion required for sustaining pregnancy compromises host defense against prenatal bacterial pathogens. Cell Host Microbe. 2011;10:54–64. [PubMed: 21767812]
12. Samstein RM, Josefowicz SZ, Arvey A, Treuting PM, Rudensky AY. Extrathymic generation of regulatory T cells in placental mammals mitigates maternal-fetal conflict. Cell. 2012;150:29–38. [PubMed: 22770213]
13. Renaud SJ, Scott RL, Chakraborty D, Rumi MA, Soares MJ. Natural killer cell deficiency alters placental development in rats. Biol Reprod. 2017;96:145–158. [PubMed: 28395334]
14. Finn CA. Implantation, menstruation and inflammation. Biol Rev Camb Philos Soc. 1986;61:313–328. [PubMed: 3542071]
15. Dekel N, Gnainsky Y, Granot I, Mor G. Inflammation and implantation. Am J Reprod Immunol. 2010;63:17–21. [PubMed: 20059465]
16. Chavan AR, Griffith OW, Wagner GP. The inflammation paradox in the evolution of mammalian pregnancy: turning a foe into a friend. Curr Opin Genet Dev. 2017;47:24–32. [PubMed: 28850905]
17. Wegmann TG, Lin H, Guilbert L, Mosmann TR. Bidirectional cytokine interactions in the maternal-fetal relationship: is successful pregnancy a TH2 phenomenon? Immunol Today. 1993;14:353–356. [PubMed: 8363725]
18. Challis JR, Lockwood CJ, Myatt L, Norman JE, Strauss JF 3rd, Petraglia F. Inflammation and pregnancy. Reprod Sci. 2009;16:206–215. [PubMed: 19208789]
19. Sykes L, MacIntyre DA, Yap XJ, Teoh TG, Bennett PR. The Th1:Th2 dichotomy of pregnancy and preterm labour. Mediators Inflamm. 2012;2012:967629.
20. Cotechini T, Komisarenko M, Sperou A, Macdonald-Goodfellow S, Adams MA, Graham CH. Inflammation in rat pregnancy inhibits spiral artery remodeling leading to fetal growth restriction and features of preeclampsia. J Exp Med. 2014;211:165–179. [PubMed: 24395887]
21. Celik H, Ayar A. Effects of erythromycin on pregnancy duration and birth weight in lipopolysaccharide-induced preterm labor in pregnant rats. Eur J Obstet Gynecol Reprod Biol. 2002;103(1):22–25. [PubMed: 12039458]
22. Lin Y, Xie M, Chen Y, Di J, Zeng Y. Preterm delivery induced by LPS in syngeneically impregnated BALB/c and NOD/SCID mice. J Reprod Immunol. 2006;71(2):87–101. [PubMed: 16797722]
23. Renaud SJ, Cotechini T, Quirt JS, Macdonald-Goodfellow SK, Othman M, Graham CH. Spontaneous pregnancy loss mediated by abnormal maternal inflammation in rats is linked to deficient uteroplacental perfusion. J Immunol. 2011;186:1799–1808. [PubMed: 21187445]
24. Silver RM, Lohner WS, Daynes RA, Mitchell MD, Branch DW. Lipopolysaccharide-induced fetal death: the role of tumor-necrosis factor alpha. Biol Reprod. 1994;50(5):1108–1112. [PubMed: 8025168]
25. Liew FY, Pitman NI, McInnes IB. Disease-associated functions of IL-33: the new kid in the IL-1 family. Nat Rev Immunol. 2010;10:103–110. [PubMed: 20081870]
26. Molofsky AB, Savage AK, Locksley RM. Interleukin-33 in tissue homeostasis, injury, and inflammation. Immunity. 2015;42: 1005–1019. [PubMed: 26084021]
27. Liew FY, Girard JP, Turnquist HR. 6 Interleukin-33 in health and disease. Nat Rev Immunol. 2016;16:676–689. [PubMed: 27640624]
28. Martin NT, Martin MU. Interleukin 33 is a guardian of barriers and a local alarmin. Nat Immunol. 2016;17:122–131. [PubMed: 26784265]
29. Cayrol C, Girard JP. Interleukin-33 (IL-33): A nuclear cytokine from the IL-1 family. Immunol Rev. 2018;281:154–168. [PubMed: 29247993]
30. Odegaard JI, Lee MW, Sogawa Y et al. Perinatal licensing of thermogenesis by IL-33 and ST2. Cell. 2016;166:841–854. [PubMed: 27453471]
31. Granne I, Southcombe JH, Snider JV et al. ST2 and IL-33 in pregnancy and pre-eclampsia. PLoS One. 2011;6:e24463.

32. Salker MS, Nautiyal J, Steel JH et al. Disordered IL-33/ST2 activation in decidualizing stromal cells prolongs uterine receptivity in women with recurrent pregnancy loss. PLoS One. 2012;7:e52252.
33. Kaitu'u-Lino TJ, Tuohey L, Tong S. Maternal serum interleukin-33 and soluble ST2 across early pregnancy, and their association with miscarriage. J Reprod Immunol. 2012;95:46–49. [PubMed: 22841163]
34. Fock V, Mairhofer M, Otti GR et al. Macrophage-derived IL-33 is a critical factor for placental growth. J Immunol. 2013;191:3734–3743. [PubMed: 23997215]
35. Topping V, Romero R, Than NG et al. Interleukin-33 in the human placenta. J Matern Fetal Neonatal Med. 2013;26:327–338. [PubMed: 23039129]
36. Hu WT, Huang LL, Li MQ, Jin LP, Li DJ, Zhu XY. Decidual stromal cell-derived IL-33 contributes to Th2 bias and inhibits decidual NK cell cytotoxicity through NF-κB signaling in human early pregnancy. J Reprod Immunol. 2015;109:52–65. [PubMed: 25712540]
37. Chakraborty D, Cui W, Rosario GX et al. HIF-KDM3A-MMP12 regulatory circuit ensures trophoblast plasticity and placental adaptations to hypoxia. Proc Natl Acad Sci USA. 2016;113: E7212–E7221. [PubMed: 27807143]
38. Scott LM, Bryant AH, Rees A, Down B, Jones RH, Thornton CA. Production and regulation of interleukin-1 family cytokines at the materno-fetal interface. Cytokine. 2017;99:194–202. [PubMed: 28712670]
39. Gokdemir IE, Ozdegirmenci O, Elmas B et al. Evaluation of ADAMTS12, ADAMTS16, ADAMTS18 and IL-33 serum levels in pre-eclampsia. J Mat-Fetal Neonatal Med. 2016;29: 2451–2456.
40. Chen H, Zhou X, Han TL, Baker PN, Qi H, Zhang H. Decreased IL-33 production contributes to trophoblast cell dysfunction in pregnancies with preeclampsia. Mediators Inflamm. 2018;2018: 9787239.
41. Romero R, Chaemsaithong P, Tarca AL et al. Maternal plasma-soluble ST2 concentrations are elevated prior to the development of early and late onset preeclampsia - a longitudinal study. J Matern Fetal Neonatal Med. 2018;31:418–432. [PubMed: 28114842]
42. Kamrani A, Rahmani SA, Mosapour P, Chavoshi R. Association of IL-33 gene rs16924159 polymorphism and recurrent pregnancy loss in Iranian Azeri women [published online ahead of print, 2020 May 7]. Horm Mol Biol. Clin Investig. 2020. 10.1515/hmbci-2020-0010
43. Huang B, Faucette AN, Pawlitz MD et al. Interleukin-33-induced expression of PIBF1 by decidual B cells protects against preterm labor. Nat Med. 2017;23:128–135. [PubMed: 27918564]
44. Ain R, Canham LN, Soares MJ. Gestation stage-dependent intrauterine trophoblast cell invasion in the rat and mouse: novel endocrine phenotype and regulation. Dev Biol. 2003;260:176–190. [PubMed: 12885563]
45. Pijnenborg R, Vercruysse L. Animal models of deep trophoblast invasion. In: Pijnenborg R, Brosens I, & Romero R, eds. Placental bed disorders: Basic science and its translation to obstetrics. Cambridge: Cambridge University Press; 2010:127–139.
46. Soares MJ, Chakraborty D, Rumi MAK, Konno T, Renaud SJ. Rat placentation: An experimental model for investigating the hemochorial maternal-fetal interface. Placenta. 2012;33:233–243. [PubMed: 22284666]
47. Ain R, Konno T, Canham LN, Soares MJ. Phenotypic analysis of the rat placenta. Methods Mol Med. 2006;121:295–313. [PubMed: 16251750]
48. Shao Y, Guan Y, Wang L et al. CRISPR/Cas-mediated genome editing in the rat via direct injection of one-cell embryos. Nat Protoc. 2014;9:2493–2512. [PubMed: 25255092]
49. Kubota K, Cui W, Dhakal P, et al. Rethinking progesterone regulation of female reproductive cyclicity. Proc Natl Acad Sci USA. 2016;113:4212–4217. [PubMed: 27035990]
50. Spicer BA, Baker RC, Hatt PA, Laycock SM, Smith H. The effects of drugs on Sephadex-induced eosinophilia and lung hyper-responsiveness in the rat. Br J Pharmacol. 1990;101:821–828. [PubMed: 1707703]
51. Matsubara S, Fushimi K, Ogawa K et al. Inhibition of pulmonary eosinophilia does not necessarily prevent the airway hyperresponsiveness induced by Sephadex beads. Int Arch Allergy Immunol. 1998;116:67–75. [PubMed: 9623512]

52. Haddad E-B, Underwood SL, Dabrowski D et al. Critical role for T cells in Sephadex-induced airway inflammation: pharmacological and immunological characterization and molecular biomarker identification. J Immunol. 2002;168:3004–3016. [PubMed: 11884473]
53. Tchernitchin A, Roorijck J, Tchernitchin X, Vandenhende J, Galand F. Dramatic early increase in uterine eosinophils after oestrogen administration. Nature. 1974;248:142–143. [PubMed: 4362086]
54. Tchernitchin X, Tchernitchin A, Galand P. Dynamics of eosinophils in the uterus after oestrogen administration. Differentiation. 1976;5:151–154. [PubMed: 184001]
55. Wang D, Ishimura R, Walia DS, et al. Eosinophils are cellular targets of the novel uteroplacental heparin-binding cytokine decidual/trophoblast prolactin-related protein. J Endocrinol. 2000;167:15–28. [PubMed: 11018749]
56. Horton MA, Larson KA, Lee JJ, Lee NA. Cloning of the murine eosinophil peroxidase gene (mEPO): characterization of a conserved subgroup of mammalian hematopoietic peroxidases. J Leukoc Biol. 1996;60:285–294. [PubMed: 8773591]
57. Nteeba J, Varberg KM, Scott RL, Simon ME, Iqbal K, Soares MJ. Poorly controlled diabetes mellitus alters placental structure, efficiency, and plasticity. BMJ Open Diabetes Res Care. 2020;8:e001243.
58. Dyer KD, Percopo CM, Rosenberg HF. IL-33 promotes eosinophilia in vivo and antagonizes IL-5-dependent eosinophil hematopoiesis ex vivo. Immunol Lett. 2013;150:41–47. [PubMed: 23246474]
59. Johnston LK, Hsu C-L, Krier-Burris RA, et al. IL-33 Precedes IL-5 in regulating eosinophil commitment and is required for eosinophil homeostasis. J Immunol. 2016;197:3445–3453. [PubMed: 27683753]
60. Johnston LK, Bryce PJ. Understanding interleukin 33 and its roles in eosinophil development. Front Med (Lausanne). 2017;4:51. [PubMed: 28512632]
61. Townsend MJ, Fallon PG, Matthews DJ, Jolin HE, McKenzie AN. T1/ST2-deficient mice demonstrate the importance of T1/ST2 in developing primary T helper cell type 2 responses. J Exp Med. 2000;191:1069–1076. [PubMed: 10727469]
62. Oboki K, Ohno T, Kajiwara N et al. IL-33 is a crucial amplifier of innate rather than acquired immunity. Proc Natl Acad Sci USA. 2010;107:18581–18586. [PubMed: 20937871]
63. Kleemann R, Deschl U, Dietmann G et al. Sephadex induced bronchial hyperreactivity in the rat: hematology, histology, histochemistry and immunohistology of the lung. Exp Toxicol Pathol. 1996;48:233–241. [PubMed: 8811289]
64. Cotechini T, Othman M, Graham CH. Nitroglycerin prevents coagulopathies and foetal death associated with abnormal maternal inflammation in rats. Thromb Haemost. 2012;107:864–874. [PubMed: 22274747]
65. Falcón BJ, Cotechini T, Macdonald-Goodfellow SK, Othman M, Graham CH. Abnormal inflammation leads to maternal coagulopathies associated with placental haemostatic alterations in a rat model of foetal loss. Thromb Haemost. 2012;107:438–447. [PubMed: 22234563]
66. Cotechini T, Hopman WJ, Graham CH. Inflammation-induced fetal growth restriction in rats is associated with altered placental morphometrics. Placenta. 2014;35:575–581. [PubMed: 24927914]
67. Robb KP, Cotechini T, Allaire C, Sperou A, Graham CH. Inflammation-induced fetal growth restriction in rats is associated with increased placental HIF-1α accumulation. PLoS One. 2017;12:e0175805.
68. Wiemers DO, Ain R, Ohboshi S, Soares MJ. Migratory trophoblast cells express a newly identified member of the prolactin gene family. J Endocrinol. 2003;179:335–346. [PubMed: 14656203]
69. Pijnenborg R, Robertson WB, Brosens I, Dixon G. Trophoblast invasion and the establishment of haemochorial placentation in man and laboratory animals. Placenta. 1981;2:71–91. [PubMed: 7010344]
70. Lee MW, Odegaard JI, Mukundan L et al. Activated type 2 innate lymphoid cells regulate beige fat biogenesis. Cell. 2015;160:74–87. [PubMed: 25543153]
71. Soares MJ, Varberg KM, Iqbal K. Hemochorial placentation: development, function, and adaptations. Biol Reprod. 2018;99:196–211. [PubMed: 29481584]

72. Wallgard E, Larsson E, He L et al. Identification of a core set of 58 gene transcripts with broad and specific expression in the microvasculature. Arterioscler Thromb Vasc Biol. 2008;28:1469–1476. [PubMed: 18483404]

73. Masiero M, Simões FC, Han HD et al. A core human primary tumor angiogenesis signature identifies the endothelial orphan receptor ELTD1 as a key regulator of angiogenesis. Cancer Cell. 2013;24:229–241. [PubMed: 23871637]

74. Tondeleir D, Vandamme D, Vandekerckhove J, Ampe C, Lambrechts A. Actin isoform expression patterns during mammalian development and in pathology: Insights from mouse models. Cell Motil Cytoskeleton. 2009;66:798–815. [PubMed: 19296487]

75. Yuan SM. α-Smooth muscle actin and ACTA2 gene expressions in vasculopathies. Braz J Cardiovasc Surg. 2015;30:644–649. [PubMed: 26934405]

76. Cross M, Mangelsdorf I, Wedel A, Renkawitz R. Mouse lysozyme M gene: isolation, characterization, and expression studies. Proc Natl Acad Sci USA. 1988;85:6232–6236. [PubMed: 3413093]

77. Choi YS, Choi HJ, Min JK et al. Interleukin-33 induces angiogenesis and vascular permeability through ST2/TRAF6-mediated endothelial nitric oxide production. Blood. 2009;114(14): 3117–3126. [PubMed: 19661270]

78. Stojkovic S, Kaun C, Basilio J et al. Tissue factor is induced by interleukin-33 in human endothelial cells: a new link between coagulation and inflammation. Sci Rep. 2016;6:25171. [PubMed: 27142573]

79. Liu J, Wang W, Wang L et al. IL-33 initiates vascular remodelling in hypoxic pulmonary hypertension by up-regulating HIF-1α and vegf expression in vascular endothelial cells. EBioMedicine. 2018;33:196–210. [PubMed: 29921553]

80. Altara R, Ghali R, Mallat Z, Cataliotti A, Booz GW, Zouein FA. Conflicting vascular and metabolic impact of the IL-33/sST2 axis. Cardiovasc. Res. 2018;114:1578–1594. [PubMed: 29982301]

81. Soares MJ. Developmental changes in the intraplacental distribution of placental lactogen and alkaline phosphatase in the rat. J Reprod Fertil. 1987;79:93–98. [PubMed: 3820187]

82. Ain R, Canham LN, Soares MJ. Dexamethasone-induced intra-uterine growth restriction impacts the placental prolactin family, insulin-like growth factor-II and the Akt signaling pathway. J Endocrinol. 2005;185:253–263. [PubMed: 15845918]

83. Bronson SL, Bale TL. Prenatal stress-induced increases in placental inflammation and offspring hyperactivity are male-specific and ameliorated by maternal anti-inflammatory treatment. Endocrinology. 2014;155:2635–2646. [PubMed: 24797632]

84. Briffa JF, Hosseini SS, Tran M, Moritz KM, Cuffe JSM, Wlodek ME. Maternal growth restriction and stress exposure in rats differentially alters expression of components of the placental glucocorticoid barrier and nutrient transporters. Placenta. 2017;59:30–38. [PubMed: 29108634]

85. Chakraborty S, Islam S, Saha S, Ain R. Dexamethasone-induced intra-uterine growth restriction impacts NOSTRIN and its downstream effector genes in the rat mesometrial uterus. Sci Rep. 2018;8:8342. [PubMed: 29844445]

86. Howerton CL, Bale TL. Prenatal programing: at the intersection of maternal stress and immune activation. Horm Behav. 2012;62:237–242. [PubMed: 22465455]

87. Bronson SL, Bale TL. The placenta as a mediator of stress effects on neurodevelopmental reprogramming. Neuropsychopharmacology. 2016;41:207–218. [PubMed: 26250599]

88. Chan JC, Nugent BM, Bale TL. Parental advisory: maternal and paternal stress can impact offspring neurodevelopment. Biol Psychiatry. 2018;83:886–894. [PubMed: 29198470]

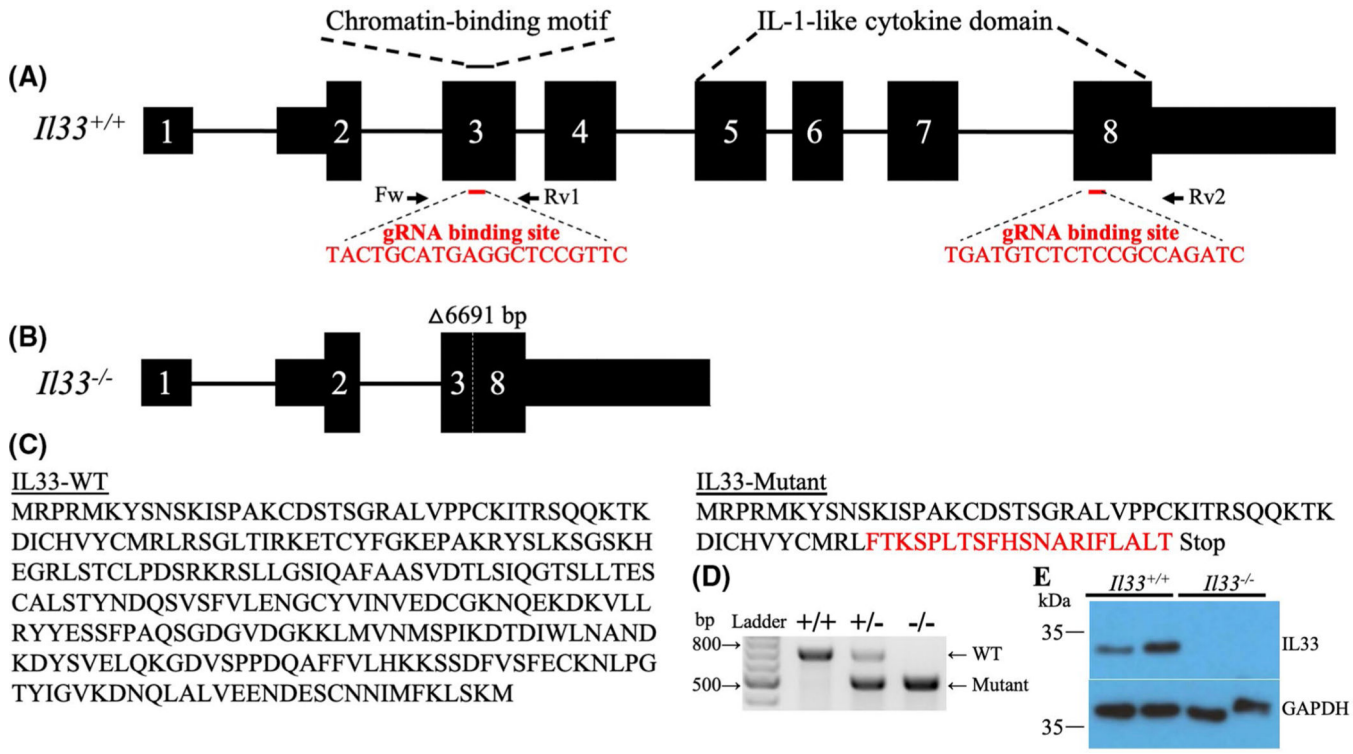

FIGURE 1.

In vivo genome editing of the rat *Il33* locus. A, Schematic representation of the rat *Il33* gene and guide RNA target sites within Exons 3 and 8 (NM_001014166.1). Red bars beneath Exons 3 and 8 correspond to the 5' and 3' crRNAs used in the genome editing. B, Mutant *Il33* allele possessing a 6,691 base pair deletion, removing part of Exons 3 and 8 and all of Exons 4–7, and leading to a frameshift and premature Stop codon in Exon 8. C, Amino acid sequences for wild-type and mutant IL33. Red sequence corresponds to the frameshift in Exon 8. D, Offspring were backcrossed to wild-type rats, and heterozygous mutant rats were intercrossed to generate homozygous mutants. Wild-type (+/+), heterozygous (+/−), and homozygous mutant (−/−) genotypes were detected by PCR. E, Western blot analysis of IL33 protein in wild-type and *Il33* null lung tissues. GAPDH was used as a loading control

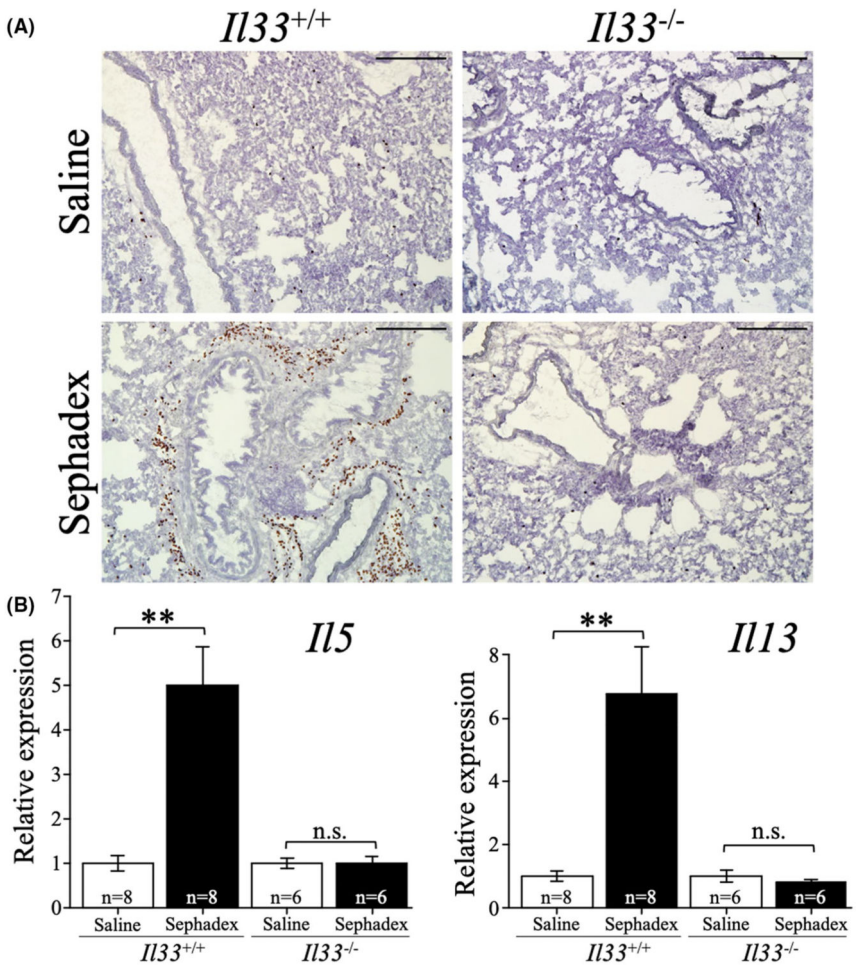

FIGURE 2.

IL33 involvement in lung inflammation. Rats were injected intravenously, via the tail vein, with saline (1 mL/animal) or Sephadex (0.5 mg/mL/animal) on days 0 and 2 and euthanized on day 5. A, Eosinophil distribution in the lungs. Eosinophils were detected histochemically by the presence of cyanide-resistant eosinophil peroxidase (EPO) activity. Scale bars = 50 μm. B, Quantitative RT-qPCR analysis of Th2 type cytokine transcripts (*Il5* and *Il13*) in the lungs (n = 6–8 animals/group). Graphs represent means ± SEM. Asterisks denote statistical difference (** $P < .01$) as determined by Student's t test. n.s. = not significant

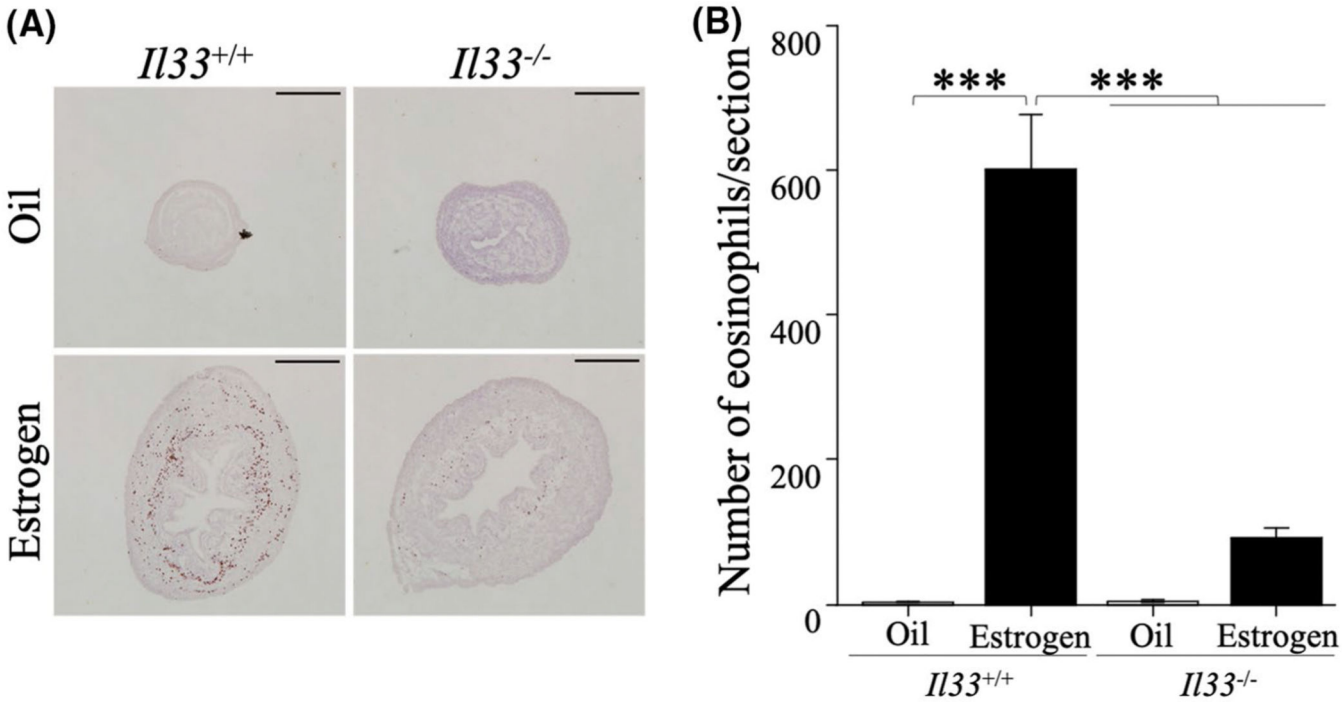

FIGURE 3.

IL33 and estrogen-induced uterine eosinophilia. Prepubertal female rats were treated subcutaneously with sesame oil (100 μL/animal) or estradiol benzoate (10 μg/100 μL sesame oil/animal) daily from postnatal day (PND) 20 through PND 22 and euthanized on PND 23. A, Eosinophil distribution in the uteri. Eosinophils were detected histochemically by the presence of cyanide-resistant eosinophil peroxidase (EPO) activity. Scale bars = 500 μm. B, The number of eosinophils per uterine section (n = 5–6 animals/group). Graphs represent means ± SEM. Asterisks denote statistical difference (***$P < .001$) as determined by Dunnett's test

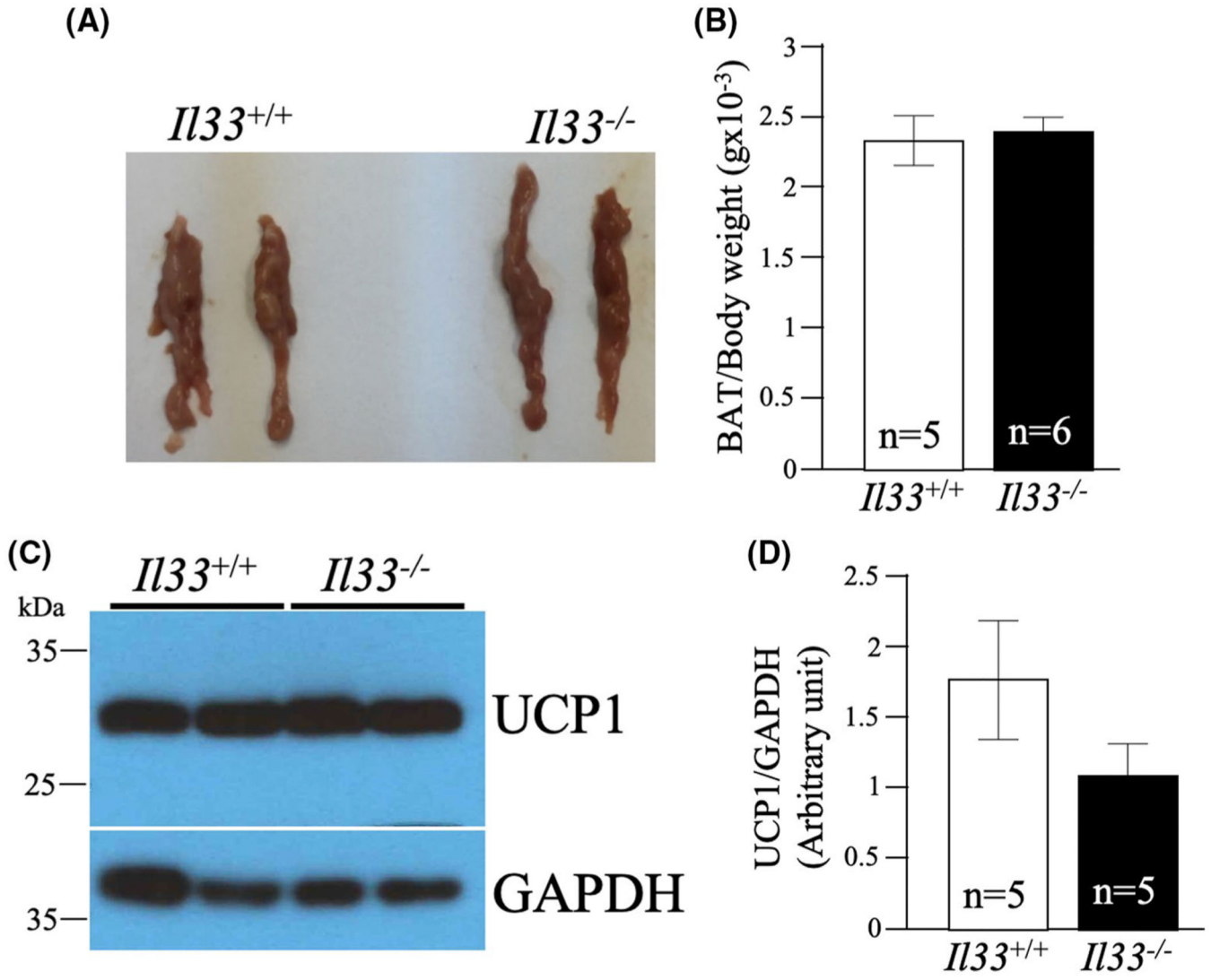

FIGURE 4.

Effects of IL33 on brown adipose tissue development. Representative gross appearance of brown adipose tissue (BAT, A) and BAT weights (B) from 3 weeks of age wild-type and *Il33*$^{-/-}$ males. C, Western blot analysis of UCP1 protein in wild-type and *Il33* null brown adipose tissues. GAPDH was used as a loading control. D, Relative protein levels of UCP1 compared to GAPDH in wild-type and *Il33* null brown adipose tissues (n = 5 animals/group). Graphs represent means ± SEM

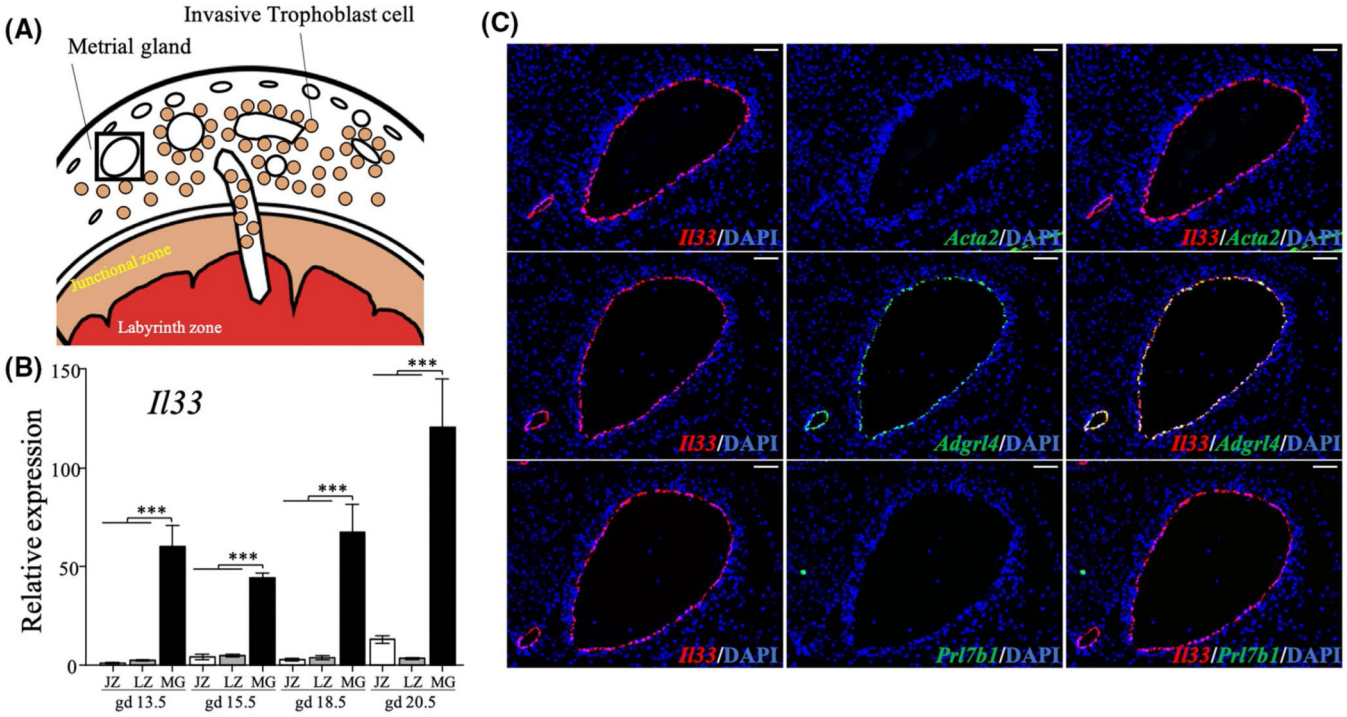

FIGURE 5.

Distribution of *Il33* transcripts within the placentation site. A, Schematic diagram of the rat placentation site highlighting the locations of the metrial gland, junctional zone, and labyrinth zone. The black box corresponds to a uterine blood vessel that is remodeled but not invaded by invasive trophoblast cells, corresponding to the microscopic fields shown in panel C. B, RT-qPCR was used to measure *Il33* transcripts in compartments of rat placentation sites during the second half of gestation (n = 6–9/group, 1 placentation site from 1 dam). Graphs represent means ± SEM. Asterisks denote statistical differences (***P < .001) as determined by Dunnett's test. JZ: junctional zone; LZ: labyrinth zone; and MG: metrial gland. C) In situ localization of transcripts for *Il33* with *Acta2* (smooth muscle cells), *Adgrl4* (endothelial cells), or *Prl7b1* (invasive trophoblast cells) in the metrial gland region at gd 17.5 of rat pregnancy. Scale bars = 100 μm. Please note the co-localization of *Il33* and *Adgrl4* transcripts, indicating endothelial cells contribute to the biosynthesis of IL33 at the uterine-placental interface

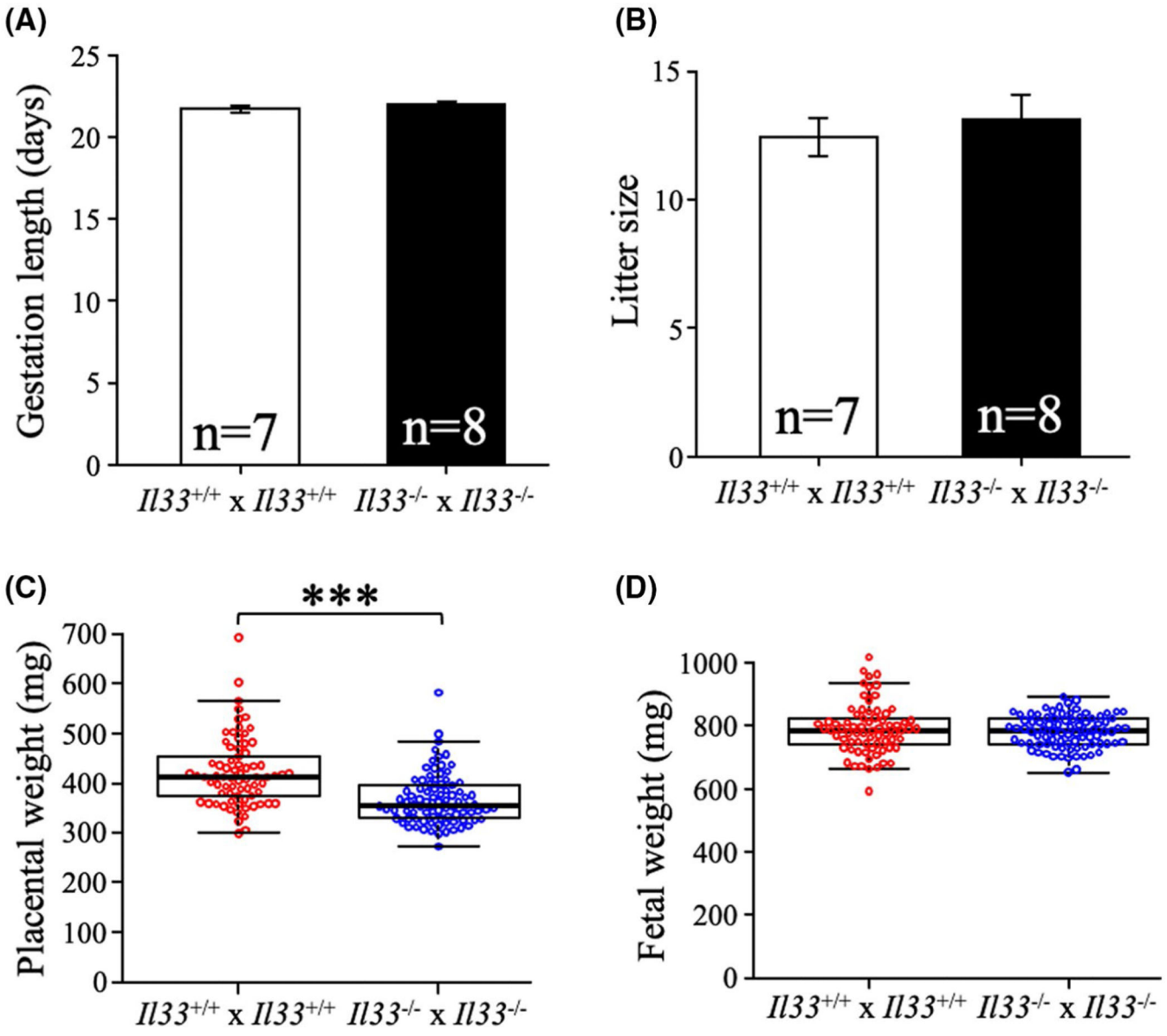

FIGURE 6.

IL33 is dispensable for pregnancy in a specific pathogen-free environment. *Il33*$^{+/+}$ and *Il33*$^{-/-}$ female rats were mated with males of the same genotype. Gestation length (A, *Il33*$^{+/+}$ x *Il33*$^{+/+}$ pregnancy, n = 7 dams, mean gestation length = 21.7 ± 0.2 vs *Il33*$^{-/-}$ x *Il33*$^{-/-}$ pregnancy, n = 8 dams, mean gestation length = 22 ± 0.2) and litter size (B, *Il33*$^{+/+}$ x *Il33*$^{+/+}$ pregnancy, n = 7 dams, mean litter size = 12.4 ± 0.7 vs *Il33*$^{-/-}$ x *Il33*$^{-/-}$ pregnancy, n = 8 dams, mean litter size = 13.1 ± 1.0) were assessed for wild-type and *Il33* homozygous mutant pregnancies. Data are presented as means ± SEM. Placental and fetal weights were measured at gestation day (gd) 17.5 (C, placental weight: *Il33*$^{+/+}$ x *Il33*$^{+/+}$, n = 73 from 6 dams, mean weight = 421.1 ± 8.2 mg vs *Il33*$^{-/-}$ x *Il33*$^{-/-}$, n = 86 from 6 dams, mean weight = 366.6 ± 5.5 mg; D, fetal weights: *Il33*$^{+/+}$ x *Il33*$^{+/+}$, n = 73 from 6 dams, mean weight = 790.1 ± 9.4 mg vs *Il33*$^{-/-}$ x *Il33*$^{-/-}$, n = 86 from 6 dams, mean weight = 782.4 ± 5.6 mg).

Data are presented as boxplots and overlaid with scatter plots. Asterisks denote statistical differences as determined by Welch's t test (***$P < .001$)

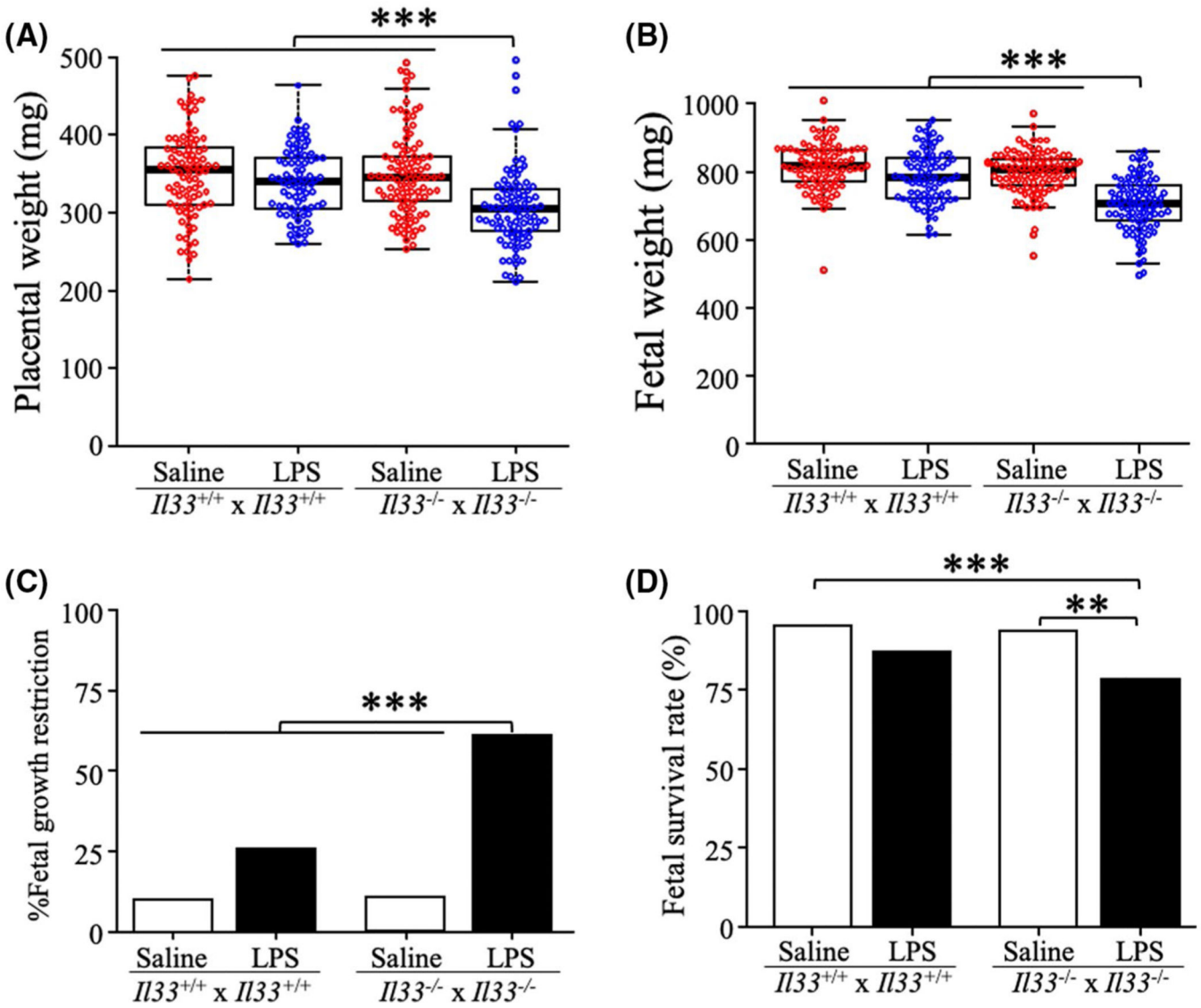

FIGURE 7.

IL33 deficient pregnancies are susceptible to the disruptive effects of lipopolysaccharide (LPS). *Il33*$^{+/+}$ and *Il33*$^{-/-}$ female rats were mated with males of the same genotype and injected intraperitoneally with saline (1 mL/kg) or LPS (10 μg/ml/kg on gestation day (gd) 13.5, and then, daily with 60 μg/ml/kg on gd 14.5, 15.5, and 16.5). Control- and LPS-treated females were sacrificed on gd 17.5. The effects of LPS on placental (A, saline-treated *Il33*$^{+/+}$ x *Il33*$^{+/+}$, n = 88 placentas from 9 dams, mean weight = 349.5 ± 6.0 mg, LPS-treated *Il33*$^{+/+}$ x *Il33*$^{+/+}$, n = 79 from 8 dams, mean weight = 338.9 ± 4.9 mg, saline-treated *Il33*$^{-/-}$ x *Il33*$^{-/-}$, n = 97 from 9 dams, mean weight = 349.4 ± 5.6 mg, and LPS-treated *Il33*$^{-/-}$ x *Il33*$^{-/-}$, n = 89 from 10 dams, mean weight = 306.2 ± 5.6 mg) and fetal (B, saline-treated *Il33*$^{+/+}$ x *Il33*$^{+/+}$, n = 88 from 9 dams, mean weight = 816.8 ± 7.5 mg, LPS-treated *Il33*$^{+/+}$ x *Il33*$^{+/+}$, n = 79 from 8 dams, mean weight = 785.0 ± 8.8 mg, saline-treated *Il33*$^{-/-}$ x *Il33*$^{-/-}$, n = 97 from 9 dams, mean weight = 797.5 ± 6.6 mg, and LPS-treated *Il33*$^{-/-}$ x *Il33*$^{-/-}$, n = 89 from 10 dams, mean weight = 703.6 ± 8.4 mg) were assessed. Data are presented as

boxplots and overlaid with scatter plots. Asterisks denote statistical difference (***$P < .001$) as determined by Dunnett's test. The effects of LPS on percent fetal growth restriction (%FGR, C) and fetal survival rate (D). A sample size of 8–10 dams/group was used in the analysis. Asterisks denote statistical differences (**$P < .01$; ***$P < .001$) as determined by Fisher's exact test with Bonferroni correction

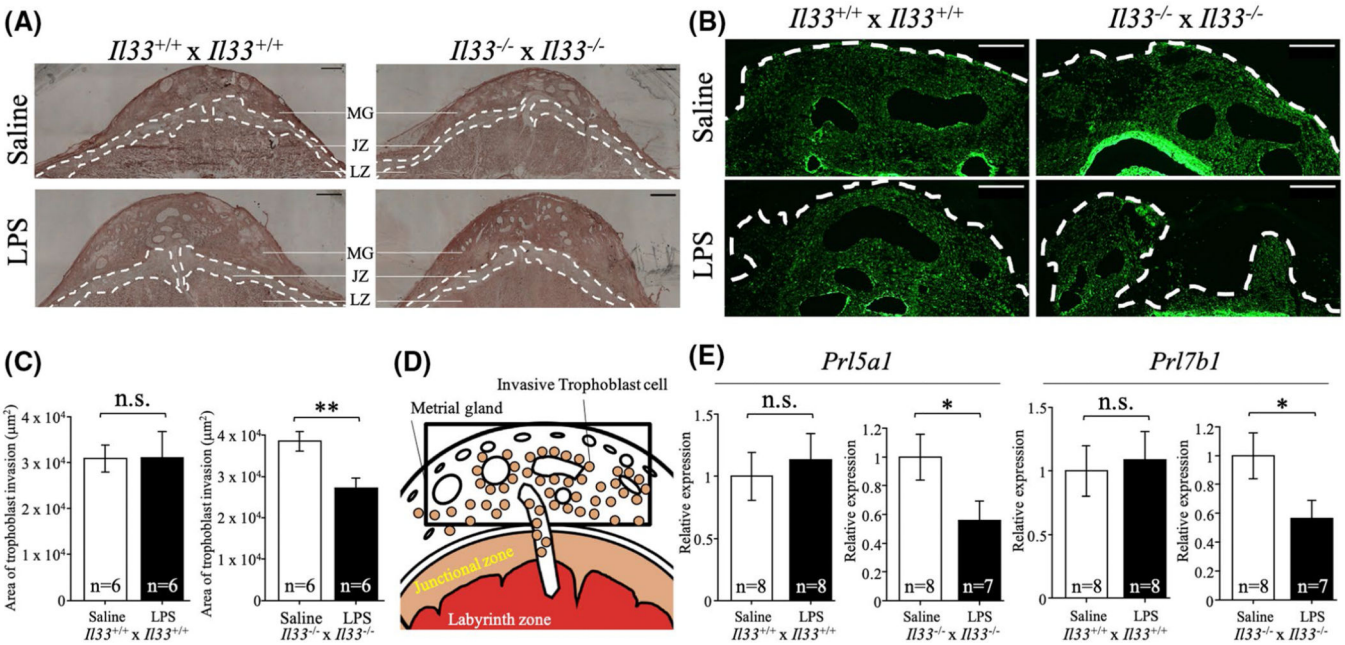

FIGURE 8.

IL33 signaling modulates lipopolysaccharide (LPS) effects on hemochorial placentation. LPS treatments were performed on pregnant *Il33*$^{+/+}$ and *Il33*$^{-/-}$ female rats as described in Figure 7. A, LPS did not dramatically affect the organization of wild-type or *Il33* null placentas into the junctional and labyrinth zone compartments. Placentation sites were immunostained for vimentin to reveal placental organization. Representative images are shown. The junctional zone compartment is demarcated using a white dashed line. Scale bars = 1000 μm. JZ: junctional zone; LZ: labyrinth zone; and MG: metrial gland. B, LPS did differentially affect wild-type vs *Il33* null intrauterine trophoblast cell invasion. Trophoblast cells were immunostained using the anti-pan-cytokeratin antibodies. Representative images are shown. The extent of intrauterine trophoblast cell invasion is demarcated using a white dashed line. Scale bars = 1000 μm. C, The area of trophoblast invasion is graphically depicted. Graphs represent means ± SEM. Asterisks denote statistical differences (**P < .01) as determined by Student's t test. n.s. = not significant. D, Schematic representation of a late gestation placentation site. The metrial gland, site for intrauterine trophoblast invasion, is highlighted in the boxed area. E, Effects of LPS on the expression of transcripts specific to invasive trophoblast cells (*Prl5a1* and *Prl7b1*) within dissected uterine-placental interface at gd 17.5 (n = 7–8 metrial glands/group, 1 metrial gland from 1 dam). Graphs represent means ± SEM. Asterisks denote statistical differences (*P < .05) as determined by Student's t test. n.s. = not significant

TABLE 1

List of primers used for RT-qPCR

Gene	Forward primers	Reverse primers	Accession no.	Amplicon size (bp)
Il5	CATGAGCACAGTGGTGAAAGAGA	TCAGTATGTCTAGCCCCTGAAAGA	NM_021834.1	149
Il13	GAGCAACATCACACAAGACCAGA	GATTCCAGGGCTGCACAGA	NM_053828.1	99
Prl5a1	TCCACACCAGACATTCCAGA	TTTCCAGGAAGCCAACATTC	NM_138527.1	143
Prl7b1	CCGTCATACTGTCTCAGCACATC	AGCTGTTGAGACCATTGACAACAA	NM_153738.1	147
Gapdh	GACATGCCGCCTGGAGAAAC	AGCCCAGGATGCCCTTTAGT	NM_017008.4	92

TABLE 2

Genotype of offspring following *Il33* heterozygous breeding

Offspring from *Il33*$^{+/-}$ × *Il33*$^{+/-}$	**Offspring genotype**		
	***Il33*$^{+/+}$**	***Il33*$^{+/-}$**	***Il33*$^{-/-}$**
Total	214	422	200
Ratio (%)	25.6	50.5	23.9